Epigenetics 10:6, 460–466; June 2015; Published with license by Taylor & Francis Group, LLC

Disruption of BRD4 at H3K27Ac-enriched enhancer region correlates with decreased c-Myc expression in Merkel cell carcinoma

Deepanwita Sengupta[1], Aarthi Kannan[2], Malan Kern[3], Mauricio A Moreno[4], Emre Vural[4], Brendan Stack Jr[4], James Y Suen[4], Alan J Tackett[1], and Ling Gao[2,*]

[1]Department of Biochemistry and Molecular Biology; University of Arkansas for Medical Sciences; Little Rock, AR USA; [2]Department of Dermatology; University of Arkansas for Medical Sciences; Little Rock, AR USA; [3]College of Medicine; University of Arkansas for Medical Sciences; Little Rock, AR USA; [4]Department of Otolaryngology-Head and Neck Surgery; University of Arkansas for Medical Sciences; Little Rock, AR USA

Keywords: BET inhibitor, BRD4, H3K27Ac, JQ1, Merkel cell carcinoma, super-enhancer

Abbreviations: MCC, Merkel cell carcinoma; BET, bromodomain and extra-terminal domain family; BRD, bromodomain; qPCR, quantitative PCR; qRT-PCR, quantitative reverse transcription PCR; ChIP, Chromatin immunoprecipitation

Pathologic c-Myc expression is frequently detected in human cancers, including Merkel cell carcinoma (MCC), an aggressive skin cancer with no cure for metastatic disease. Bromodomain protein 4 (BRD4) regulates gene transcription by binding to acetylated histone H3 lysine 27 (H3K27Ac) on the chromatin. Super-enhancers of transcription are identified by enrichment of H3K27Ac. BET inhibitor JQ1 disrupts BRD4 association with super-enhancers, downregulates proto-oncogenes, such as *c-Myc*, and displays antitumor activity in preclinical animal models of human cancers. Here we show that an enhancer proximal to the *c-Myc* promoter is enriched in H3K27Ac and associated with high occupancy of BRD4, and coincides with a putative *c-Myc* super-enhancer in MCC cells. This observation is mirrored in tumors from MCC patients. Importantly, depleted BRD4 occupancy at the putative *c-Myc* super-enhancer region by JQ1 correlates with decreased c-Myc expression. Thus, our study provides initial evidence that super-enhancers regulate c-Myc expression in MCC.

Introduction

Merkel cell carcinoma (MCC) is a rare but aggressive skin cancer with a rising incidence.[1] Although MCC is less common than cutaneous melanoma, its disease-associated mortality rate is higher than that of melanoma. The standard treatment is surgery with or without adjuvant radiation.[2] Nevertheless, no targeted therapy exists for metastatic diseases.[2] Thus, it is imperative to understand the underlying molecular events and find a cure for this devastating cancer.

Intense mutational analysis reveals no significant contribution of major signaling pathways to MCC pathogenesis. Studies have eventuated the discovery of Merkel cell polyomavirus (MCV); however, the pathogenic role of MCV remains uncertain.[3] Although multiple microarray studies have provided insights into MCC pathogenesis, molecular events essential to MCC pathogenesis are largely unknown.[4-6] Though the principal tenet in cancer is that tumor is initiated and driven by mutations, it is now clear that epigenetic pathways also play a significant role in oncogenesis. Moreover, diverse gene mutations generally converge functionally to deregulate similar core cellular process, which can be targeted by approaching epigenetic vulnerabilities.

Bromodomains (BRDs) are protein domains involved in acetylation-dependent assembly of transcriptional regulator complexes. BRD4, along with BRD2, BRD3, and testes/oocyte-specific BRDT, constitute the bromodomain and extra-terminal (BET) domain family of proteins in mammals.[7] Participation of bromodomains in oncogenic rearrangement is exemplified in NUT midline carcinoma (NMC). Moreover, an oncogenic *BRD4-NUT* fusion gene driven by *BRD4* promoter is found in NMC and other types of human cancers.[8] Furthermore, inhibition of BET bromodomain by small-molecule compounds with high potency against BET proteins, such as JQ1, results in significant downregulation of c-Myc as well as other transcription factors, and display antitumor activity in a variety of preclinical animal models of human cancers.[9-12] Importantly, these studies

*Correspondence to: Ling Gao; Email: LGao@uams.edu
Submitted: 12/22/2014; Revised: 02/20/2015; Accepted: 03/19/2015
http://dx.doi.org/10.1080/15592294.2015.1034416

have established the feasibility of BET inhibition within an acceptable therapeutic window of tolerability. As a result, similar small molecules are currently in Phase I clinical trial for haematopoietic malignancies and advanced solid tumors (ClinicalTrials.gov Identifier NCT01587703, NCT01713582, NCT01949883, NCT01987362, and NCT01943851).

Enhancers are DNA regulatory elements and are key regulators of tissue-specific gene transcription. Accordingly, super-enhancers are larger clusters of transcriptional enhancers with high levels of several different histone acetylation marks, especially H2K27Ac.[13] Similar to other bromodomain proteins, such as BRD2 and BRD3, BRD4 has also been shown to associate with chromatin via interaction with different histone acetylation marks, such as H4K5, H4K8, H4K12, H3K9, H3K14, H4K16, and H3K27.[13–17] Of these, BRD4 bound H3K27Ac sites have been associated with very high gene activity.[16] Emerging data links disruption of super-enhancers with inhibitory oncogene transcription that often exhibits high levels of BRD4 occupancy at nearby enhancer/super-enhancer regions, such as *c-Myc* in haematopoietic malignancies.[13] Interestingly, we and another group have found that pathologic c-Myc amplification is common in MCC.[18,19] Moreover, we have also shown that JQ1 represses tumor growth in xenograft MCC mouse models, suggesting an epigenetic mechanism in regulating key oncogene expressions in MCC.[18] In this study, we sought to investigate the potential role of super-enhancers in regulating c-Myc overexpression in MCC. Taking advantage of chromatin immunoprecipitation coupled with real-time or quantitative PCR (ChIP-qPCR), we examined the co-occupancy of H3K27Ac and BRD4 at the putative *c-Myc* super-enhancer in MCC. We have demonstrated relative high co-occupancies of H3K27Ac and BRD4 in a putative *c-Myc* super-enhancer region in MCC cells with pathologic c-Myc amplification, and further confirmed our finding in tumor samples from MCC patients. Next, we have shown that the disruption of BRD4 at the putative *c-Myc* super-enhancer region correlates with suppressed c-Myc expression and repressed tumor growth in JQ1 treated xenograft tumors. Thus, our study has provided initial evidence of super-enhancer as a regulatory mechanism in c-Myc expression in MCC.

Results and Discussion

c-Myc overexpressing MCC cells show high occupancy of H3K27Ac and BRD4 in a putative *c-Myc* super-enhancer region

While there is an increasing appreciation of the contribution of epigenetic pathways in oncogenesis, limited parallel studies have been conducted in MCC. We have previously shown that c-Myc overexpression is common in MCC.[18] Here, we wanted to investigate the mechanism involved in regulating c-Myc expression in MCC. At first, we assessed the relative protein and mRNA levels of c-Myc in 4 primary human MCC cell lines. MCC-3 and MCC-5 were established in our laboratory.[20] MKL-1 and MKL-2 were a gift from Dr. Becker (University of Graz, Austria).[21] All four MCC cell lines grew in suspension in culture and expressed characteristic markers of MCC as described previously.[18] Both immunoblotting and quantitative reverse transcription PCR (qRT-PCR) demonstrated a significantly higher expression of c-Myc in MCC-3 and MCC-5 cells as compared to that in MKL-1 and MKL-2 cells (**Figs. 1A and B**). The putative super-enhancer (reported in Materials and Methods) was identified as a region proximal to the *c-Myc* promoter with high levels of H3K27Ac and low levels of H3K4me3 (characteristic features of super-enhancers)[13] in 7 human cancer cell lines (GM12878, H1-hESC, HSMM, HUVEC, K562, NHEK, NHLF) reported by The Encyclopedia of DNA Elements (ENCODE) project in the UCSC genome browser [Human Feb. 2009 (GRCh37/hg19) Assembly[22]]. Consistently, the putative super-enhancer region (Chr8:128,700,000–129,000,000) is also located in close proximity to *c-Myc* super-enhancers identified in other cancers like glioblastoma, breast, prostate, and pancreatic cancer (Supplementary **Fig. 1**).[15] Control regions were chosen as 5000 base pair (bp) upstream and downstream of the putative *c-Myc* super-enhancer region. It has been shown that super-enhancers are correlated with higher levels of occupancy of both H3K27Ac and BRD4.[13] Therefore, we performed ChIP using antibodies against H3K27Ac followed by qPCR using primers targeting the putative super-enhancer region of *c-Myc*, to determine the relative enrichment of H3K27Ac in 4 MCC cell lines (**Fig. 1C**). A relatively high level of H3K27Ac was detected at the region proximal to the *c-Myc* promoter in c-Myc overexpressing MCC-3 and MCC-5 cells, indicating that the region harbored a putative super-enhancer of *c-Myc* in MCC cells. Next, to determine the co-occupancy of BRD4 at that region, a ChIP was performed using antibody against BRD4 followed by qPCR using primers targeting the putative super-enhancer region in all MCC cell lines. As shown in **Figure 1D**, a significantly higher occupancy of BRD4 was detected at the putative super-enhancer region in both MCC-3 and MCC-5 cell lines with pathologic c-Myc amplification, as compared to MKL-1 and MKL-2 cell lines with basal c-Myc expression. BRD4 levels from total MCC cell lysates were similar in all MCC cell lines tested (**Fig. 1A**), suggesting that the higher c-Myc expression is not due to a global increase in the level of the transcriptional activator BRD4 but rather specific enrichment at the *c-Myc* putative super-enhancer region. This indicates that this putative super-enhancer may play a role in regulating c-Myc expression via providing more docking sites for BRD4 and further recruiting other transcriptional activators, which ultimately leads to higher c-Myc expression.

To validate our finding, we analyzed fresh tumors from MCC patients. Based on our previous findings, we have selected a total of 5 human MCC tumors in which c-Myc expression was examined by immunoblotting using an antibody against c-Myc.[18] Three tumors (tumors #11, #12 and #16) overexpressed c-Myc, whereas 2 tumors (tumor #10 and #15) had basal c-Myc expression.[18] We analyzed these 5 tumors for relative enrichment of H3K27Ac and BRD4 at the putative *c-Myc* super-enhancer region. As shown in **Figure 2**, MCC tumors with c-Myc overexpression showed a greater H3K27Ac level coupled with a higher

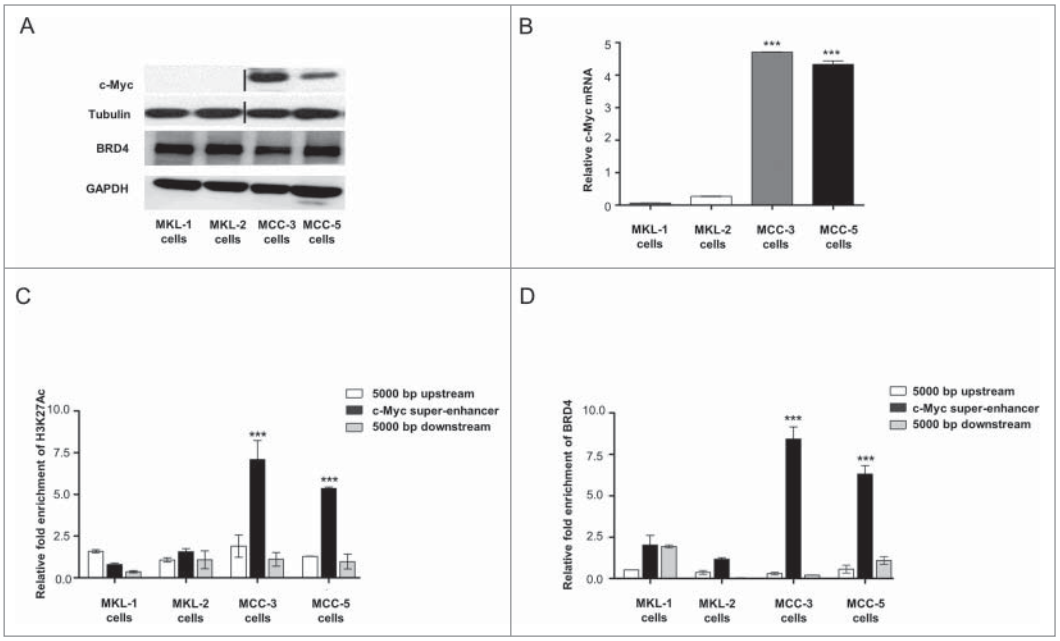

Figure 1. Myc over-expressing cell lines exhibit enrichment of H3K27Ac and BRD4 at the *c-Myc* putative super-enhancer region. (**A**) Immunoblotting demonstrates c-Myc overexpression in MCC-3 and MCC-5 cells, and similar BRD4 levels in all MCC cells. Tubulin and GAPDH have been used as loading control for immunoblotting. In the c-Myc immunoblot, the black dividing line separates images grouped from different parts of the same blot. (**B**) qRT-PCR analysis shows elevated levels of c-Myc transcription in MCC-3 and MCC-5 cells. The mRNA expression of c-Myc has been normalized to that of MRPS2. (*** $P < 0.001$) indicates significantly higher levels of c-Myc transcripts. (**C-D**) Chromatin immunoprecipitation performed in MCC cell lines followed by qPCR analysis using primers of putative *c-Myc* super-enhancer regions demonstrates a higher co-occupancy of H3K27Ac and BRD4 at the *c-Myc* putative super-enhancer region. In the graphs, relative enrichment represents average fold enrichment of the target promoter in immunoprecipitation (IP) vs. input, normalized to β-*actin*. The total histone H3 ChIP signal has been used to normalize H3K27Ac ChIP signal. Regions of 5000 base pairs (bp) upstream and downstream to the target sequence were used as controls to ensure that the enrichment is specific to the target sequence. (***$P < 0.001$) indicates significant enrichment in MCC-3 and MCC-5 cells. In all the graphs, data is presented as mean ± SEM of 3 independent experiments, where SEM is standard error mean represented by the error bar.

BRD4 enrichment at the putative *c-Myc* super-enhancer region, reinforcing our hypothesis that super-enhancers serve as a potential mechanism in regulating c-Myc expression in MCC.

Disruption of BRD4 at the putative *c-Myc* super-enhancer region by BET inhibitor JQ1 correlates with decreased c-Myc expression in MCC-3 xenograft tumors

The pleiotropic effects of targeting epigenetic writers (DNA methyltransferase) and epigenetic erasers (histone deacetylase inhibitors) have hampered their broader application in oncology. The recently developed bromodomain BET inhibitors, such as JQ1, that target the protein-protein interaction modules of enhancer/super-enhancers, have provided more effective epigenetic approaches to cancer treatment. Using a xenograft MCC mouse model, we have previously demonstrated that JQ1 inhibits tumor growth.[18] Moreover, greater inhibition of tumor growth following JQ1 treatment was found in MCC tumors with c-Myc overexpression, such as in xenograft tumors derived form MCC-3 cells.[18] To investigate whether the JQ1-mediated tumor repression occurs via disruption of BRD4 at the putative *c-Myc* super-enhancer region, we used 2 xenograft mouse models. The MCC-3 (cells with c-Myc overexpression) xenograft mouse model has been described previously.[18] The control group used in this study was the MKL-1 (cells with basal c-Myc expression) xenograft mouse model. As described previously, a mixture of matrigel and MKL-1 cells (2×10^7) was injected subcutaneously on the rear flanks of NOD-SCIDγ (NSG) mice. When xenograft tumors approached ~100 mm^3 in volume (or 7 mm in diameter), NSG mice bearing xenograft tumors were randomized into 2 groups and treatment was initiated with intraperitoneal administration of 50 mg/kg/day JQ1 or vehicle for a 3-week duration, respectively. NSG mice treated with JQ1 had no obvious signs of toxicity (based on body weight, food and water intake, activity, and general exam). Mice bearing MKL-1 xenograft tumors were sacrificed after completion of 21-day treatment. JQ1 induced a 48.9% reduction in MKL-1 xenograft tumors as compared to a 75.6% reduction in MCC-3 tumors, suggesting that JQ1 exerted a greater antitumor effect in MCC-3 xenografts with c-Myc overexpression relative to control MKL-1 xenografts with basal c-Myc expression (**Fig. 3A**). Moreover, JQ1 decreased c-Myc expression in MCC-3 xenograft tumors, as detected by immunoblotting and qRT-PCR (**Figs. 3B and C**). Very low c-Myc expression was detected in control MKL-1 xenografts (**Figs. 3B and C**), consistent with our observation in MKL-1 cell line (**Figs. 1A and B**). Sustained BRD4 and H3K27Ac levels were found in MCC-3 xenograft tumor lysates between the treatment and control groups, suggesting that c-Myc inhibition by JQ1 has no effect on overall BRD4 and H3K27Ac levels (**Fig. 3B**). Importantly, JQ1 treatment selectively depleted BRD4 enrichment at the *c-Myc* putative super-enhancer region in MCC-3 xenograft (**Fig. 3D**). As this is accompanied by suppressed MCC-3 xenograft tumor growth (**Fig. 3A**) and decreased c-Myc expression (**Figs. 3B and C**), taken together, we have provided the initial evidence that super-enhancers play a potential role in regulating c-Myc expression in MCC. Next, we silenced BRD4 expression by introduction of BRD4 shRNA into MCC-3 cells, as described

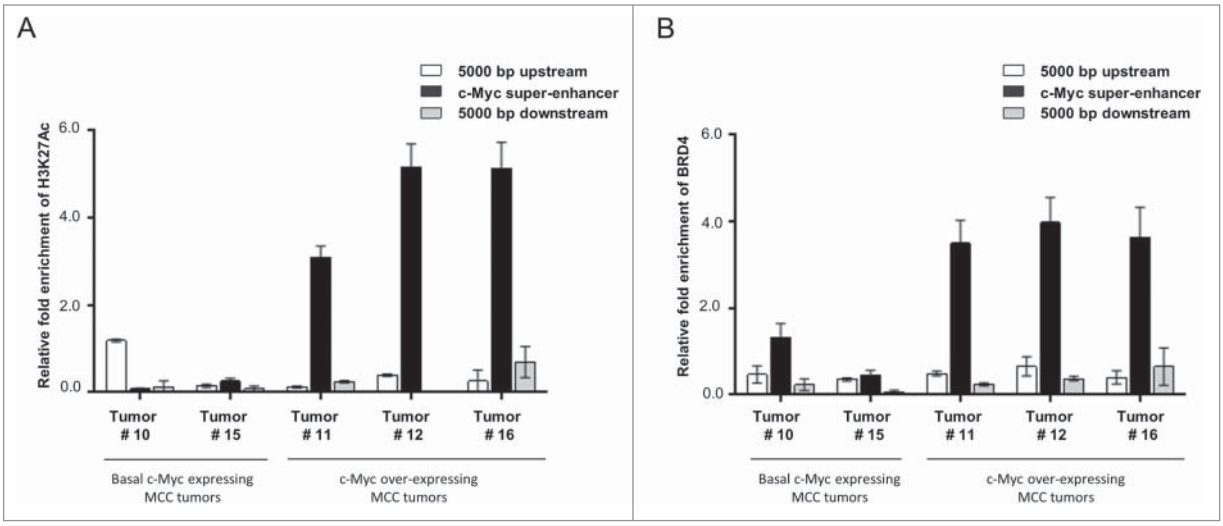

Figure 2. Human MCC tumors with c-Myc overexpression are associated with high levels of H3K27Ac and BRD4 occupancy at the *c-Myc* putative super-enhancer region. (**A-B**) ChIP-qPCR reveals that MCC tumors with c-Myc overexpression (Tumor #11, #12 and #16) show higher co-occupancy of H3K27Ac and BRD4 at the putative *c-Myc* super-enhancer region as compared to tumors with basal c-Myc expression (Tumor #10 and #15). Regions of 5000 base pairs (bp) upstream and downstream to the target sequence were used as controls to ensure that the enrichment is specific to the target sequence. Relative enrichment is the average fold enrichment of the target promoter in IP vs. input, normalized to β-*actin*. ChIP signal for H3K27Ac is normalized to total H3. Data is presented as mean ± SEM, where SEM is standard error mean of triplicate analysis represented by the error bar.

previously.[18] MCC-3 cells transduced with scramble shRNA served as control. More than 40% reduction of BRD4 was observed in MCC-3 knockdown cells by qPCR (Supplementary **Fig. 2A**). By ChIP-qPCR, impaired BRD4 recruitment was found in putative super-enhancer region in BRD4 knockdown MCC-3 cells as compared to that in the control (Supplementary **Fig. 2B**).

In this study, we have demonstrated enrichment of BRD4 and H3K27Ac at a putative *c-Myc* super-enhancer region in both MCC-3 and MCC-5 cells exhibiting pathologic c-Myc amplification. Similar observations were made in c-Myc over-expressing tumors from MCC patients. Taking advantage of our xenograft MCC mouse models, we have shown that disruption of BRD4 by JQ1 at the putative *c-Myc* super-enhancer region correlates with decreased c-Myc expression and suppressed MCC-3 xenograft tumor growth. Our work adds MCC to the emerging themes in the complex picture of *c-Myc* regulation by enhancers/super-enhancers.

Elucidating functional importance of super-enhancers is an area of ongoing research that continues to enhance our understanding of the molecular pathogenesis of cancer. Super-enhancers not only regulate the expression of critical genes in certain human cancers, but also control cell identity, such as in embryonic stem cell.[14,23] Moreover, super-enhancers are tumor type specific.[14] Furthermore, DNA translocation, transcription factor overexpression, and focal amplification occur frequently in cancer, and these mechanisms can account for the ability of cancer cells to acquire super-enhancers.[14] A recent study has shown that an oncogenic super-enhancer forms through somatic mutation in a noncoding intergenic region and contributes to tumorigenesis in a subset of T cell acute lymphoblastic leukemia.[24] Additionally, enhancer activity has been linked to resistance to Notch inhibitor in T-cell leukemia.[25] Finally, emerging data suggests enhancer RNAs play a role in regulation of gene expression.[26-28] Further characterization of the endogenous super-enhancers by ChIP-seq will identify potential key genes that control Merkel cell state, key oncogenes/tumor suppressor genes that function in the acquisition of hallmark capabilities in MCC tumorigenesis, and biomarkers to direct the treatment.

Materials and Methods

Cell culture

MCC cell lines MCC-3 and MCC-5 have been established in our laboratory and are derived from the lymph node metastases of MCC patients, in accordance with University of Arkansas for Medical Sciences (UAMS) Institutional Review Board (IRB) approvals for human study protocol.[20] MKL-1 and MKL-2 cell lines are gifts from DR Becker (University of Graz, Austria). All the MCC cells were cultured with RPMI-1640 medium supplemented with 10% fetal bovine serum (FBS) and 10% penicillin-streptomycin-L-glutamine and incubated at 37°C in a humidified incubator with 5% CO2. Fresh medium was added every other day.

Lentiviral transduction

Lentivector directing expression of shRNA specific to BRD4 (TRCN0000318771) was purchased from Sigma-Aldrich

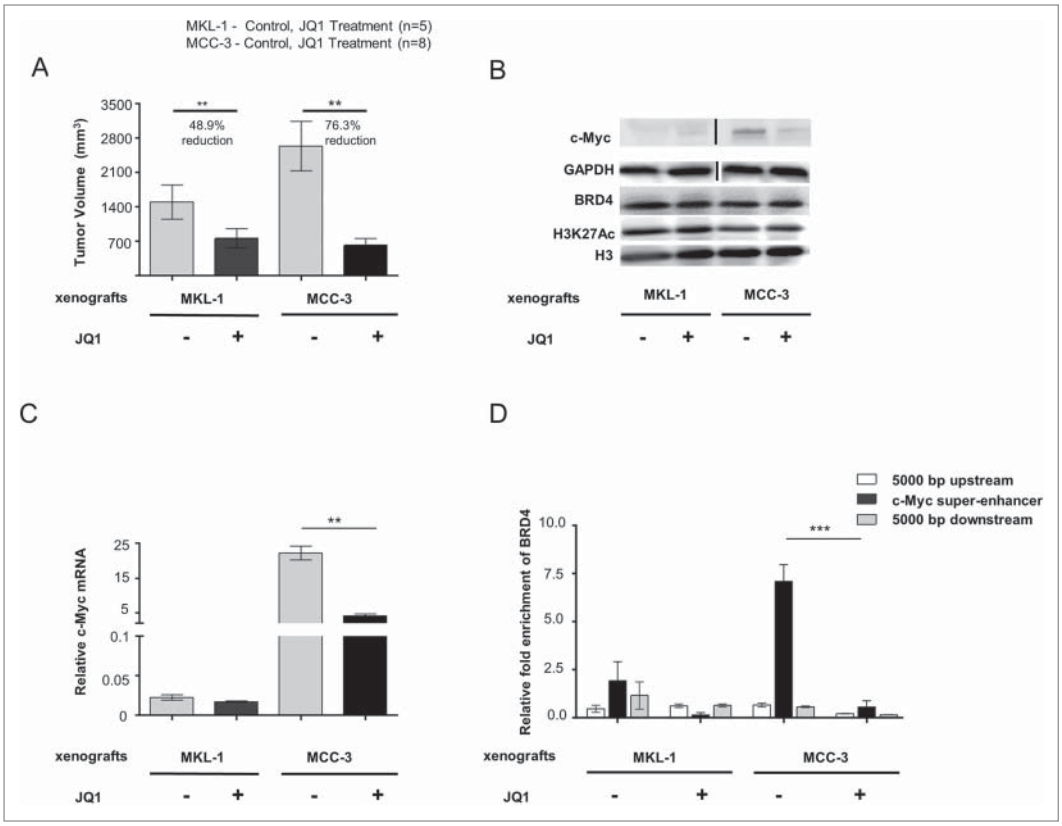

Figure 3. BET inhibitor JQ1 depletes BRD4 enrichment at the *c-Myc* putative super-enhancer region in MCC-3 xenograft tumors. (**A**) Significant suppression of tumor growth are detected in both MCC-3 (**$P < 0.01$) and MKL-1 (*$P < 0.1$) xenograft tumors. A greater reduction of tumor growth is observed in MCC-3 xenograft tumors with c-Myc overexpression (75.6% vs. 48.9%). Data is presented as final tumor volume ± SEM from tumor bearing NSG mice treated with vehicle or JQ1. (**B-C**) JQ1 significantly reduced c-Myc expression in MCC-3 xenograft tumors as demonstrated by representative immunoblotting (**B**) and qRT-PCR analysis (**C**) (**$P < 0.01$ vs. vehicle treatment) of 3 biological replicates. In the c-Myc immunoblot, the black dividing line separates images grouped from different parts of the same blot. The c-Myc mRNA expression has been normalized to that of MRPS2. (**D**) JQ1 depletes BRD4 occupancy at the putative *c-Myc* super-enhancer regions in MCC-3 xenograft tumors by ChIP-qPCR analysis (***$P < 0.001$ vs. vehicle treatment). Regions of 5000 base pairs (bp) upstream and downstream to the target sequence were used as controls to ensure that the enrichment is specific to the target region. Relative enrichment represents average fold enrichment of the target promoter in IP vs. input, normalized to β-*actin*. ChIP signal for H3K27Ac is normalized to total H3. Data is presented as mean ± SEM. Error bars in the graph represent SEM from independent analysis of 3 biological replicates. (+) and (−) represents drug (JQ1) and vehicle treatment, respectively.

(#SHCLNG). The non-targeting PLKO.1 scramble shRNA (plasmid 1864) was purchased from Addgene. The lentiviral transduction was performed as described previously.[18] Briefly, to generate recombinant lenti-viruses, 293T/17 cells were co-transfected with gene transfer vectors and virus packaging vectors, ΔH8.2 and VSVG using TransIT-LT1 transfection reagent. Virus supernatants were collected 48 h after transfection. MCC cell lines were transduced with virus supernatant for 48 h in fibronectin-coated 6-well plates in the presence of 8 μg/ml polybrene after spinocculation at 800 g, 32°C for 30 min.

Xenograft studies

MKL-1 xenograft mouse models were generated as described previously.[18] Briefly, tumor-bearing NSG mice (The Jackson Laboratory, strain #5557) were randomized into treatment and control groups ($n \geq 7$ for each condition) and began receiving intraperitoneal injection (i.p.) administration of vehicle (10% 2-Hydroxypropyl-β-cyclodextrin in water) or 50 mg/kg/day JQ1 (Selleck Chemicals, #S7110) for 3 weeks. Mice were monitored daily, tumor xenografts were measured with digital calipers, and tumor volume was calculated as $L^2 \times W/2$, where L is length and W is width. At experimental endpoints, mice were euthanized via isoflurane followed by cervical dislocation, and tumors were excised and dissected for histology characterization and further mechanistic studies. All animal experiments were done under a protocol approved by University of Arkansas for Medical Sciences (UAMS) Institutional Animal Care and Use Committee. In accordance with institutional guidelines on animal care, experimental endpoints were determined by one of the following: (1) completion of twenty-one day treatment course, or (2) attainment of tumor burden exceeding 2 cm in any dimension, or (3) further complications affecting animal welfare. Upon reaching experimental endpoints, mice were humanely euthanized, and tumors were excised and dissected for characterization and mechanistic studies.

Immunoblotting

Whole cell protein lysates were prepared from cultured cells and resolved by SDS-PAGE. Proteins were transferred onto Immobilon polyvinylidene difluoride (PVDF) membrane (EMD Millipore, #IPVH00010), pre-soaked in methanol, by electroblotting at 200V for 2 h at room temperature. Membrane was blocked in 5% milk (1X TBST) for 1 h at room temperature. Membrane was then incubated with primary antibody in 5% milk overnight at 4°C, and finally probed with secondary antibody in 5% milk for 1 h at room temperature. Detection was

performed using Western Lightning Plus ECL enhanced chemiluminescent substrate (Perkin-Elmer Inc., #NEL103001EA) according to manufacturer's instructions. For probing, the following antibodies were used: anti-GAPDH (Cell signaling Technology, #5174), anti-c-Myc (Cell signaling Technology, #9402), anti-tubulin (Sigma, #T9026), anti-BRD4 (Cell signaling Technology, #13440), anti-Histone H3 (Abcam, #ab1791), anti-Histone H3K27Ac (Abcam, #ab4729), ECL Rabbit IgG, HRP-linked (GE Healthcare Life Sciences, #NA934V), goat anti-mouse IgG-HRP (Santa Cruz biotechnology, #sc-2005). Images were obtained using ImageQuant LAS 4000 imager (GE Healthcare, Pittsburgh, PA). The images were obtained as tiff files.

Gene expression analysis

Total RNA was isolated from all 4 MCC cell lines and xenografts MCC tumors derived form MCC-3 and MKL-1 with a RNeasy kit (Qiagen, #74104). cDNA was generated from mRNA using a Reverse Transcription Kit (Applied Biosystems, #4368814). Quantitative reverse transcription PCR (qRT-PCR) was performed with a StepOne Plus Real-Time PCR System (Applied Biosystems, Foster City, CA). The following TaqMan Gene Expression Assays primers were used: Hs00905030_m1 (c-Myc) and Hs00211334_m1 (MRPS2). Triplicate runs of each sample were normalized to MRPS2 mRNA to determine relative expression.

Chromatin immunoprecipitation

Chromatin immunoprecipitation (ChIP) experiment was performed in cells, frozen xenograft tumors, and frozen MCC patient tumors. All of these were cross-linked using 1% formaldehyde for 10 min followed by quenching with 0.125 M glycine for 5 min. Cross-linked cells were lysed using lysis buffer (50 mM Hepes pH 7.5, 140 mM NaCl, 1 mM EDTA, 1% triton X-100, 0.1% sodium deoxycholate, 1 tablet of Roche protease inhibitor per 10 mL lysis buffer). The whole cell lysates were sonicated for 30 min on max setting using a Bioruptor^{TM} UCD-200 (Diagenode, Denville, NJ). Sonicated lysates were then centrifuged at 2500 g for 10 min, and the supernatant was used to perform ChIP using M280 sheep anti-rabbit IgG Dynabeads® (Life Technologies, #11203D), according to manufacturer's instructions. The ChIP antibodies used were BRD4 antibody (Cell Signaling Technology, #13440) and H3 (Abcam, #ab1791) and H3K27Ac antibodies (Abcam, #ab4729). For quantification of enrichment of BRD4 and H3K27Ac (normalized to histone H3) at specific promoter regions, qPCR was performed using a reaction mixture containing 1X SsoAdvanced SYBR Green Supermix (Bio-Rad, #172–5270), primers (0.33 μM) and DNA (100ng). The cyclic conditions used were 95°C for 2 min, followed by 45 cycles at 95°C for 15 s and 50°C for 20 s. Fold changes were determined using a MiniOpticon real-time PCR detection system (Bio-Rad, Hercules, CA). Following primers were ordered from Integrated DNA Technologies (IDT) and used for real-time analysis:

For targeting putative *c-Myc* super-enhancer region,

c-Myc forward (5′- GGACCCGCTTCTCTGAAAGG-3′), and

c-Myc reverse (5′-GCAAGTGGACTTCGGTGCTTACC-3′),

For targeting a control region 5000 bp upstream of *c-Myc* super-enhancer region,

control 5000 bp upstream forward (5′-CAGAAGG-CAACTTCCATG-3′), and

control 5000 bp upstream reverse (5′-CCTGAAAGTGGTTCTTAATACTG-3′),

For targeting a control region 5000 bp downstream of *c-Myc* super-enhancer region,

control 5000 bp downstream forward (5′-CCATAATG-TAAACTGCCTC-3′), and

control 5000 bp downstream reverse (5′-CAGAGAAA-CATTGTGTAAATC-3′).

Following primer set was used for normalization:

β-actin forward (5′-CTTGGCATCCACGAAACTA-3′), and

β-actin reverse (5-′GAGCCAGAGCAGTGATCTCC-3′).

The use of patient tumors in the study was approved by the Institutional Review Board (IRB) of University of Arkansas for Medical Sciences (UAMS) and informed consent was obtained from each patient before inclusion in the study.

Statistical analysis

For in vivo studies, all values are represented as mean ± standard error mean (SEM). Statistical analysis was performed using Mann-Whitney t-test and $^{*}P$-value < 0.05 was considered statistically significant. For *in vitro* studies, all the experiments were performed in biological as well as technical triplicates. All values in the graphs represent mean ± SEM by student t-test.

Disclosure of Potential Conflicts of Interest

No potential conflicts of interest were disclosed.

Acknowledgments

The content is solely the responsibility of the authors and does not necessarily represent the official views of the NIH.

Funding

The project described was supported by the Translational Research Institute (TRI), grants UL1TR000039 and KL2TR000063 through the NIH National Center for Research

Resources and the National Center for Advancing Translational Sciences. This study was also supported by funds from the Department of Dermatology, the Winthrop P. Rockefeller Cancer Institute, University of Arkansas for Medical Sciences, and the Arkansas Biosciences Institute, the major research component of the Arkansas Tobacco Settlement Proceeds Act of 2000. AJT acknowledges support from R01GM106024, R33CA173264, P30GM103450, and P20GM103429.

Supplemental Material

Supplemental data for this article can be accessed on the publisher's website.

References

1. Iyer JG, Storer BE, Paulson KG, Lemos B, Phillips JL, Bichakjian CK, Zeitouni N, Gershenwald JE, Sondak V, Otley CC, et al. Relationships among primary tumor size, number of involved nodes, and survival for 8044 cases of Merkel cell carcinoma. J Am Acad Dermatol 2014; 70:637-43; PMID:24521828; http://dx.doi.org/10.1016/j.jaad.2013.11.031
2. Hughes MP, Hardee ME, Cornelius LA, Hutchins LF, Becker JC, Gao L. Merkel cell carcinoma: epidemiology, target, and therapy. Curr Dermatol Rep 2014; 3:46-53; PMID:24587977; http://dx.doi.org/10.1007/s13671-014-0068-z
3. Schrama D, Peitsch WK, Zapatka M, Kneitz H, Houben R, Eib S, Haferkamp S, Moore PS, Shuda M, Thompson JF, et al. Merkel cell polyomavirus status is not associated with clinical course of Merkel cell carcinoma. J Invest Dermatol 2011; 131:1631-8; PMID:21562568; http://dx.doi.org/10.1038/jid.2011.115
4. Paulson KG, Lemos BD, Feng B, Jaimes N, Peñas PF, Bi X, Maher E, Cohen L, Leonard JH, Granter SR, et al. Array-CGH reveals recurrent genomic changes in Merkel cell carcinoma including amplification of L-Myc. J Invest Dermatol 2009; 129:1547-55; PMID:19020549; http://dx.doi.org/10.1038/jid.2008.365
5. Paulson KG, Iyer JG, Tegeder AR, Thibodeau R, Schelter J, Koba S, Schrama D, Simonson WT, Lemos BD, Byrd DR, et al. Transcriptome-wide studies of merkel cell carcinoma and validation of intratumoral CD8+ lymphocyte invasion as an independent predictor of survival. J Clin Oncol 2011; 29:1539-46; PMID:21422430; http://dx.doi.org/10.1200/JCO.2010.30.6308
6. Harms PW, Patel RM, Verhaegen ME, Giordano TJ, Nash KT, Johnson CN, Daignault S, Thomas DG, Gudjonsson JE, Elder JT, et al. Distinct gene expression profiles of viral- and nonviral-associated merkel cell carcinoma revealed by transcriptome analysis. J Invest Dermatol 2013; 133:936-45; PMID:23223137; http://dx.doi.org/10.1038/jid.2012.445
7. Shi J, Vakoc CR. The mechanisms behind the therapeutic activity of BET bromodomain inhibition. Mol Cell 2014; 54:728-36; PMID:24905006; http://dx.doi.org/10.1016/j.molcel.2014.05.016
8. Evans AG, French CA, Cameron MJ, Fletcher CD, Jackman DM, Lathan CS, Sholl LM. Pathologic characteristics of NUT midline carcinoma arising in the mediastinum. Am J Surg Pathol 2012; 36:1222-7; PMID:22790861; http://dx.doi.org/10.1097/PAS.0b013e318258f03b
9. Filippakopoulos P, Knapp S. Targeting bromodomains: epigenetic readers of lysine acetylation. Nat Rev Drug Discov 2014; 13:337-56; PMID:24751816; http://dx.doi.org/10.1038/nrd4286
10. Filippakopoulos P, Qi J, Picaud S, Shen Y, Smith WB, Fedorov O, Morse EM, Keates T, Hickman TT, Felletar I, et al. Selective inhibition of BET bromodomains. Nature 2010; 468:1067-73; PMID:20871596; http://dx.doi.org/10.1038/nature09504
11. Asangani IA, Dommeti VL, Wang X, Malik R, Cieslik M, Yang R, Escara-Wilke J, Wilder-Romans K, Dhanireddy S, Engelke C, et al. Therapeutic targeting of BET bromodomain proteins in castration-resistant prostate cancer. Nature 2014; 510:278-82; PMID:24759320; http://dx.doi.org/10.1038/nature13229
12. Delmore JE, Issa GC, Lemieux ME, Rahl PB, Shi J, Jacobs HM, Kastritis E, Gilpatrick T, Paranal RM, Qi J, et al. BET bromodomain inhibition as a therapeutic strategy to target c-Myc. Cell 2011; 146:904-17; PMID:21889194; http://dx.doi.org/10.1016/j.cell.2011.08.017
13. Lovén J, Hoke HA, Lin CY, Lau A, Orlando DA, Vakoc CR, Bradner JE, Lee TI, Young RA. Selective inhibition of tumor oncogenes by disruption of super-enhancers. Cell 2013; 153:320-34; PMID:Can't; http://dx.doi.org/10.1016/j.cell.2013.03.036
14. Hnisz D, Abraham BJ, Lee TI, Lau A, Saint-André V, Sigova AA, Hoke HA, Young RA. Super-enhancers in the control of cell identity and disease. Cell 2013; 155:934-47; PMID:24119843; http://dx.doi.org/10.1016/j.cell.2013.09.053
15. Zhang W, Prakash C, Sum C, Gong Y, Li Y, Kwok JJ, Thiessen N, Pettersson S, Jones SJ, Knapp S, et al. Bromodomain-containing protein 4 (BRD4) regulates RNA polymerase II serine 2 phosphorylation in human CD4+ T cells. J Biol Chem 2012; 287:43137-55; PMID:23086925; http://dx.doi.org/10.1074/jbc.M112.413047
16. Zippo A, Serafini R, Rocchigiani M, Pennacchini S, Krepelova A, Oliviero S. Histone crosstalk between H3S10ph and H4K16ac generates a histone code that mediates transcription elongation. Cell 2009; 138:1122-36; PMID:19766566; http://dx.doi.org/10.1016/j.cell.2009.07.031
17. Hargreaves DC, Horng T, Medzhitov R. Control of inducible gene expression by signal-dependent transcriptional elongation. Cell 2009; 138:129-45; PMID:19596240; http://dx.doi.org/10.1016/j.cell.2009.05.047
18. Shao Q, Kannan A, Lin Z, Stack BC, Suen JY, Gao L. BET protein inhibitor JQ1 attenuates Myc-amplified MCC tumor growth in vivo. Cancer Res 2014; 74:7090-102; PMID:25277525; http://dx.doi.org/10.1158/0008-5472.CAN-14-0305
19. Kwun HJ, Shuda M, Feng H, Camacho CJ, Moore PS, Chang Y. Merkel cell polyomavirus small T antigen controls viral replication and oncoprotein expression by targeting the cellular ubiquitin ligase SCFFbw7. Cell Host Microbe 2013; 14:125-35; PMID:23954152; http://dx.doi.org/10.1016/j.chom.2013.06.008
20. Lin Z, McDermott A, Shao L, Kannan A, Morgan M, Stack BC, Moreno M, Davis DA, Cornelius LA, Gao L. Chronic mTOR activation promotes cell survival in Merkel cell carcinoma. Cancer Lett 2014; 344:272-81; PMID:24262658; http://dx.doi.org/10.1016/j.canlet.2013.11.005
21. Hafner C, Houben R, Baeurle A, Ritter C, Schrama D, Landthaler M, Becker JC. Activation of the PI3K/AKT pathway in Merkel cell carcinoma. PLoS One 2012; 7:e31255; PMID:22363598; http://dx.doi.org/10.1371/journal.pone.0031255
22. Kent WJ, Sugnet CW, Furey TS, Roskin KM, Pringle TH, Zahler AM, Haussler D. The human genome browser at UCSC. Genome Res 2002; 12:996-1006; PMID:12045153; http://dx.doi.org/10.1101/gr.229102
23. Di Micco R, Fontanals-Cirera B, Low V, Ntziachristos P, Yuen SK, Lovell CD, Dolgalev I, Yonekubo Y, Zhang G, Rusinova E, et al. Control of embryonic stem cell identity by BRD4-dependent transcriptional elongation of super-enhancer-associated pluripotency genes. Cell Rep 2014; 9:234-47; PMID:25263550; http://dx.doi.org/10.1016/j.celrep.2014.08.055
24. Mansour MR, Abraham BJ, Anders L, Berezovskaya A, Gutierrez A, Durbin AD, Etchin J, Lawton L, Sallan SE, Silverman LB, et al. An oncogenic super-enhancer formed through somatic mutation of a noncoding intergenic element. Science 2014; 346:1373-7; PMID:25394790; http://dx.doi.org/10.1126/science.1259037
25. Yashiro-Ohtani Y, Wang H, Zang C, Arnett KL, Bailis W, Ho Y, Knoechel B, Lanauze C, Louis L, Forsyth KS, et al. Long-range enhancer activity determines Myc sensitivity to Notch inhibitors in T cell leukemia. Proc Natl Acad Sci U S A 2014; 111:E4946-53; PMID:25369933; http://dx.doi.org/10.1073/pnas.1407079111
26. Ren B. Transcription: enhancers make non-coding RNA. Nature 2010; 465:173-4; PMID:20463730; http://dx.doi.org/10.1038/465173a
27. Lam MT, Li W, Rosenfeld MG, Glass CK. Enhancer RNAs and regulated transcriptional programs. Trends Biochem Sci 2014; 39:170-82; PMID:24674738; http://dx.doi.org/10.1016/j.tibs.2014.02.007
28. Lai F, Shiekhattar R. Enhancer RNAs: the new molecules of transcription. Curr Opin Genet Dev 2014; 25:38-42; PMID:24480293; http://dx.doi.org/10.1016/j.gde.2013.11.017